Biomimetic Electrochemistry

A Biomimetic Pathway for Hydrogen Evolution from a Model of the Iron Hydrogenase Active Site**

Sascha Ott, Mikael Kritikos, Björn Åkermark, Licheng Sun, and Reiner Lomoth**

The recent elucidation of the structures of two iron hydrogenases isolated from different organisms[1,2] has provided a unique insight into the active site of these hydrogen-producing enzymes. This knowledge has fueled intense research aimed at the synthesis of close mimics of the active site that can achieve catalytic activities comparable to that found in the natural system.[3] The particular interest in this system arises from the fact that the enzyme relies exclusively on readily available iron cations in the active site.[4] Apart from a thiolate-linked $[Fe_4S_4]$ cluster, cyanide and carbonyl ligands populate the whole coordination sphere of the two iron nuclei in the site, which are within bonding distance of one another and are additionally connected by a nonproteic dithiolate bridge.[5–7] Although a subject of some controversy in the past, recent spectroscopic, crystallographic, and theoretical studies suggest the structure of this tether is S-CH_2-NH-CH_2-S (azadithiolate, ADT).[8,9] The importance of the nitrogen heteroatom in the disulfide bridge arises from its potential for protonation in its position close to the active site, which offers a thermodynamically and kinetically favorable pathway for hydrogen evolution in the natural system. Model complexes that exhibit catalytic features related to those of the iron hydrogenases have so far relied solely on propyldithiolate (PDT) bridges. For example, Rauchfuss and co-workers demonstrated that $[(\mu\text{-PDT})Fe_2(CO)_4PMe_3(CN)]^-$ serves as a catalyst for electrochemical hydrogen evolution,[10,11] and Darensbourg and co-workers have reported that $[(\mu\text{-H})(\mu\text{-PDT})Fe_2(CO)_4(PMe_3)_2]^+$ is a catalyst for H_2/D_2 scrambling.[12] In these models, the electron-donating cyanide

[*] Dr. S. Ott, Prof. Dr. B. Åkermark, Dr. L. Sun
Department of Organic Chemistry
Arrhenius Laboratory, Stockholm University
10691 Stockholm (Sweden)
Fax: (+46) 8-154-908
E-mail: sascha.ott@organ.su.se

Dr. R. Lomoth
Department of Physical Chemistry
BMC, Uppsala University
BOX 579, 75123 Uppsala (Sweden)
Fax: (+46) 18-471-3654
E-mail: reiner.lomoth@fki.uu.se

Dr. M. Kritikos
Department of Structural Chemistry
Arrhenius Laboratory, Stockholm University
10691 Stockholm (Sweden)

[**] We thank Fernando Lopes Pinto (Uppsala University) for his help with the hydrogen GC analysis. Financial support for this work was provided by the Swedish Energy Agency, the Knut and Alice Wallenberg Foundation, and the Swedish Research Council (VR).

  DOI: 10.1002/ange.200353190

and phosphane ligands are crucial because they increase the electron density of the Fe^{I}–Fe^{I} bond and thereby facilitate protonation at this position.[13] In our approach, which involves light-driven proton reduction by utilizing a suitable photosensitizer,[14] such electronegative ligands are counterproductive as they shift the reduction potential of the respective diiron complex to more negative values and render electron transfer to this site unfavorable.[15] Once the first examples of mimics containing the azadithiolate (ADT) tether had been made available by us[14] and others,[16–18] we anticipated that an alternative, more biomimetic pathway for catalytic evolution of hydrogen may be accessible that involves the nitrogen heteroatom of the bridge acting as a basic site and allows electronically unfavorable ligands to be omitted.

To investigate this possibility, [(μ-ADT)$Fe_2(CO)_6$] (**1**; ADT = S-CH_2-NR-CH_2-S, R = *p*-bromobenzyl) was synthesized by a procedure similar to that previously used for the synthesis of analogous complexes.[14,17] The bromide functionality on the aromatic ring in complex **1** acts as a synthetic handle for the attachment of further redox-active components. Single-crystal x-ray diffraction analysis of **1** (Figure 1)[19] reveals the usual distorted square-pyramidal geometry around the iron centers.[14,16–18] In contrast to the crystal structures of phenyl-substituted ADT-bridged diiron complexes,[14] the benzyl moiety in that of **1** resides in a pseudo-equatorial position relative to the metalloheterocycle, with the nitrogen lone-pair pointing towards an iron nucleus. In the solid state, the nonbonding C···N distance between the ADT nitrogen atom and the nearest carbonyl carbon atom is significantly shorter in **1** than in the phenyl-substituted analogues (3.02 and 3.5 Å, respectively). After protonation of **1**, the proton is anticipated to be in proximity to the diiron active site. Protonation of **1** to form $\mathbf{1H^+}$ occurs in an acetonitrile solution upon addition of a strong acid such as triflic, hydrochloric, or perchloric acid.[20] The resonances in the ^{1}H NMR spectrum (CD_3CN) of $\mathbf{1H^+}$ are generally shifted to lower magnetic field strengths than those in **1**; the protons in proximity to the nitrogen atom are displaced by 0.64 and 0.31 ppm, respectively. The carbonyl frequencies in the IR spectrum of $\mathbf{1H^+}$ are shifted 15 cm^{-1} higher in energy relative to those of **1**, which is consistent with observations made during the protonation of a related complex.[18] Protonation of **1** is accompanied by a color change from orange to yellow. The UV absorption maximum is shifted from 328 to 332 nm, and during titration with acid an isosbestic point is preserved at 320 nm, which indicates the formation of a single protonation product at all acid concentrations (Figure 2).[21]

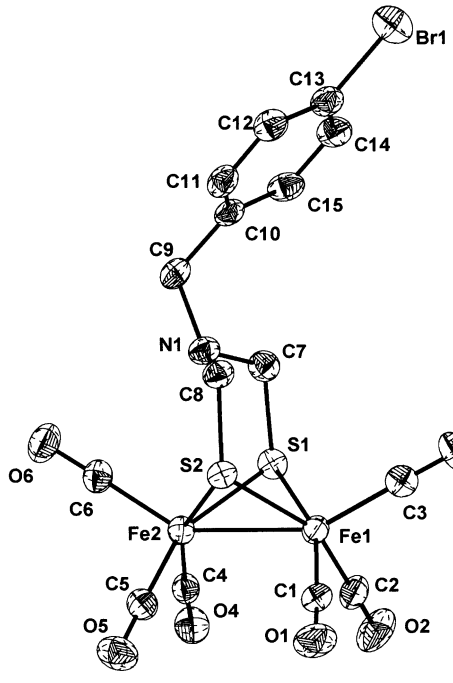

Figure 1. ORTEP view (ellipsoids at 30% probability level) of $C_{15}H_{10}BrFe_2NO_6S_2$ (**1**). Selected bond lengths [Å]: Fe1–Fe2 2.5083(7), Fe1–S1 2.2460(12), Fe1–S2 2.2526(10), Fe2–S1 2.2573(10), Fe2–S2 2.2682(10), Fe1–C1 1.785(5), Fe1–C2 1.791(4), Fe1–C3 1.803(4), Fe2–C4 1.790(4), Fe2–C5, 1.778(4), Fe2–C6 1.804(4), N1–C7 1.433(5).

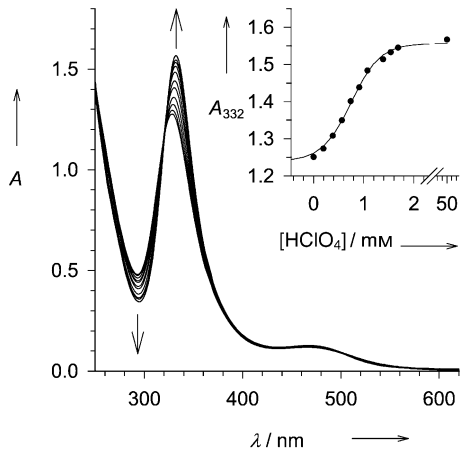

Figure 2. UV/Vis spectra (l = 1 mm) of **1** (1 mM) in acetonitrile. Arrows indicate spectral changes upon addition of increasing amounts of acid (concentrations as shown in the inset). Inset: absorbance at λ = 332 nm as a function of acid concentration.

The reduction behavior of **1** and $\mathbf{1H^+}$ was investigated by cyclic and differential pulse voltammetry. In dry acetonitrile, electrochemically irreversible one-electron reduction of **1** occurs at −1.56 V versus the ferrocene/ferrocenium couple (Fc/Fc^+; Figure 3a and inset).[22] Addition of excess perchloric acid to a 1 mM solution of **1** in acetonitrile resulted in the cyclic voltammogram of $\mathbf{1H^+}$ being observed. The first reduction peak is shifted by around 400 mV towards more positive potential, which is consistent with the introduced positive charge.[23] The position of this peak is independent of the acid concentration[21] and corresponds to a one-electron reduction of the protonated complex to **1H**. Following this reduction, a second reduction peak occurs around −1.4 V, the height of which increases and which shifts to more negative potential with increasing acid concentration (Figure 3a, inset). Both of these features are indicative of catalytic proton reduction,[24] which is also supported by the observation of gas evolution at this potential. Analysis of the reaction

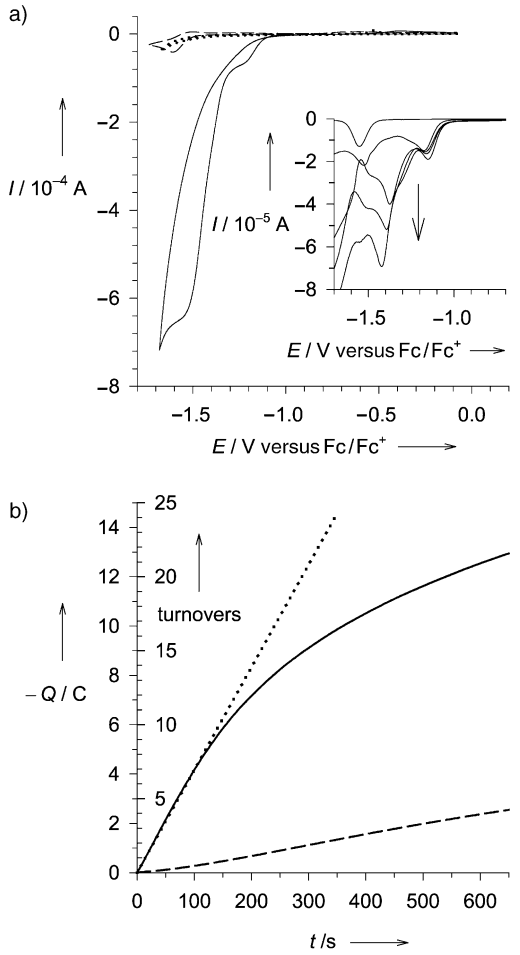

Figure 3. a) Cyclic voltammograms ($\nu = 0.100\ V s^{-1}$) of **1** (-----), $HClO_4$ (50 mM; •••••), and **1** in the presence of $HClO_4$ (50 mM; ——); inset: differential pulse voltammograms of **1** in the presence of increasing acid concentrations (0, 10, 30, 50, 70 mM) as indicated by the arrow; working electrode: glassy carbon; surface area: 0.07 cm^2. b) Coulometry for bulk electrolysis of $HClO_4$ (50 mM) at a graphite electrode in the presence of **1** (——) and without **1** (-----); extrapolation of the catalytic reduction at the initial electrolysis rate (•••••); electrolysis potential: −1.48 V; volume: 3 mL; electrode surface area: 1.4 cm^2. All measurements were made on 1 mM solutions of **1** in CH_3CN, with $(Bu)_4NPF_6$ (0.1 M) as the supporting electrolyte. All potentials given are versus Fc/Fc^+.

by gas chromatography showed hydrogen to be the sole gaseous product. Without the diiron complex, reduction of protons at the carbon electrode is slow at the potential of the second reduction peak.

Further evidence for the catalytic activity of **1** was obtained when solutions of **1** with excess perchloric acid were electrolyzed at −1.48 V, a potential slightly beyond the second reduction peak (Figure 3b). When the cell is loaded with a 1 mM solution of **1** containing 50 mM perchloric acid, the initial rate of electrolysis is more than 10 times higher than that in the absence of the catalyst, and 9 F (based on the amount of **1**) pass through the cell in 1 minute, which corresponds to 4.5 turnovers. The rate of electrolysis slows down as the proton concentration decreases and after approximately 10 minutes the total charge passed through the cell approaches its maximum of 50 F, which is equivalent to 25 turnovers. Once the current has dropped during electrolysis, the initial value can be recovered by replacing the consumed protons.

Based on the structural, spectroscopic, and electrochemical data described above, we propose the catalytic cycle shown in Scheme 1. After protonation, $\mathbf{1H^+}$ is electrochemically reduced to **1H** at −1.18 V. We anticipate that the reduction increases the electron density of the Fe^I–Fe^I bond and creates a situation similar to that achieved by the presence of electron-donating cyanide and phosphane ligands in other model complexes.[11,12] The electron-rich Fe–Fe bond is then available for protonation, which leads to $\mathbf{1H_2^+}$. This protonation enables the complex to undergo a second reduction at around −1.4 V, molecular hydrogen is then released, and the catalyst is liberated and made available for another cycle.

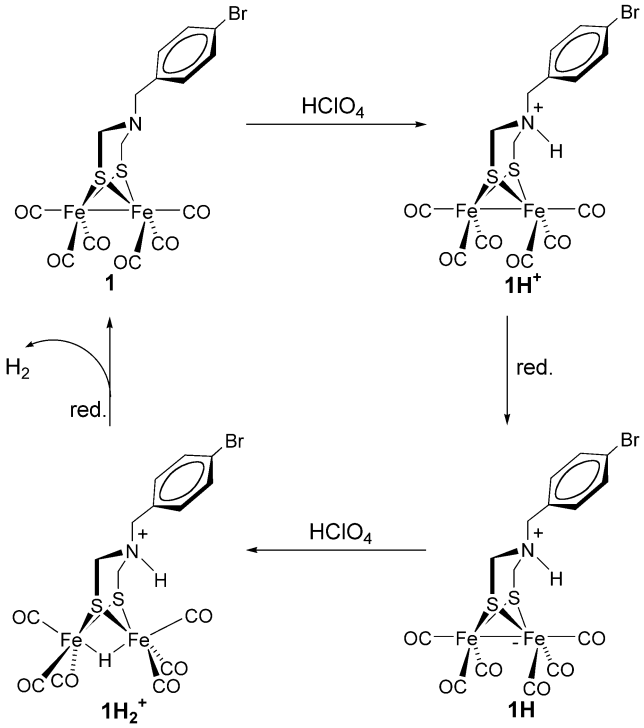

Scheme 1. Proposed catalytic cycle for the electrochemical reduction of protons in the presence of **1**.

Electrochemical production of hydrogen catalyzed by a mimic of the iron hydrogenase active site has been reported once before, with a potential of −1.2 V versus Ag/AgCl (corresponding to −1.71 V versus Fc/Fc^+)[25] required to drive the reduction of protons.[10] Omission of electron-withdrawing ligands at the diiron site and utilization of the basicity of the ADT nitrogen atom enabled us to shift this potential by 230 mV to a more positive value and thus make this reduction significantly easier. The shift in potential can be rationalized by considering the altered catalytic mechanism, which in our system commences with the protonation of the ADT nitrogen atom. In this way, the catalytic cycle proposed for **1** resembles the natural system more closely than other reported models.

With a mimic of the iron hydrogenase active site that operates at a moderately negative potential, we are currently pursuing the incorporation of **1** into a device capable of using the action of light to drive the evolution of hydrogen.

Experimental Section

1: Reaction of *p*-bromobenzylamine,[26] *p*-CH_2O, thionylchloride, and the lithium salt of diironhexacarbonyldisulfide[27] on a 0.5-mmol scale gave 151 mg (0.27 mmol, 54%) of **1** as a red solid. Elemental analysis (%): calcd for $C_{15}H_{10}BrFe_2NO_6S_2$: C 32.40, H 1.81, N 2.52; found: C 32.44, H 1.99, N 2.52; ^{1}H NMR (300 MHz, CD_3CN): $\delta = 7.48$ (d, $J =$ 8.4 Hz, 2H), 7.12 (d, $J = 8.4$ Hz, 2H), 3.72 (s, 2H), 3.40 ppm (s, 4H); ^{13}C NMR (75 MHz, $CDCl_3$): $\delta = 207.7$, 134.9, 131.8, 130.3, 121.8, 61.2, 52.3 ppm; IR (CH_3CN): $\tilde{\nu} = 2074$, 2036, 1997 cm^{-1} (C=O); UV/Vis (CH_3CN): 328 (12800), 465 nm ($1200\,M^{-1}cm^{-1}$).

1H$^+$: ^{1}H NMR (300 MHz, CD_3CN): $\delta = 7.65$ (d, $J = 8.4$ Hz, 2H), 7.36 (d, $J = 8.4$ Hz, 2H), 4.36 (s, 2H), 3.71 ppm (very broad, 4H); ^{13}C NMR (75 MHz, CD_3CN): $\delta = 206.9$, 134.7, 133.6, 126.9, 125.9, 64.2, 49.4 ppm; IR (CH_3CN): $\tilde{\nu} = 2089$, 2052, 2016 cm^{-1} (C=O); UV/Vis (CH_3CN): 332 (15700), 465 nm ($1200\,M^{-1}cm^{-1}$).

Received: October 30, 2003 [Z53190]

Keywords: bioinorganic chemistry · biomimetic catalysis · electrochemistry · hydrogen · iron hydrogenase

[1] J. W. Peters, W. N. Lanzilotta, B. J. Lemon, L. C. Seefeldt, *Science* **1998**, *282*, 1853 – 1858.
[2] Y. Nicolet, C. Piras, P. Legrand, E. C. Hatchikian, J. C. Fontecilla-Camps, *Structure* **1999**, *7*, 13 – 23.
[3] J. Alper, *Science* **2003**, *299*, 1686 – 1687.
[4] M. Y. Darensbourg, E. J. Lyon, J. J. Smee, *Coord. Chem. Rev.* **2000**, *206–207*, 533 – 561.
[5] M. Frey, *ChemBioChem* **2002**, *3*, 152 – 160.
[6] J. W. Peters, *Curr. Opin. Struct. Biol.* **1999**, *9*, 670 – 676.
[7] Y. Nicolet, B. J. Lemon, J. C. Fontecilla-Camps, J. W. Peters, *Trends Biochem. Sci.* **2000**, *25*, 138 – 143.
[8] H.-J. Fan, M. B. Hall, *J. Am. Chem. Soc.* **2001**, *123*, 3828 – 3829.
[9] Y. Nicolet, A. L. de Lacey, X. Vernede, V. M. Fernandez, E. C. Hatchikian, J. C. Fontecilla-Camps, *J. Am. Chem. Soc.* **2001**, *123*, 1596 – 1602.
[10] F. Gloaguen, J. D. Lawrence, T. B. Rauchfuss, M. Benard, M.-M. Rohmer, *Inorg. Chem.* **2002**, *41*, 6573 – 6582.
[11] F. Gloaguen, J. D. Lawrence, T. B. Rauchfuss, *J. Am. Chem. Soc.* **2001**, *123*, 9476 – 9477.
[12] X. Zhao, I. P. Georgakaki, M. L. Miller, R. Mejia-Rodriguez, C.-Y. Chiang, M. Y. Darensbourg, *Inorg. Chem.* **2002**, *41*, 3917 – 3928.
[13] M. S. Arabi, R. Mathieu, R. Poilblanc, *J. Organomet. Chem.* **1979**, *177*, 199 – 209.
[14] S. Ott, M. Kritikos, B. Åkermark, L. Sun, *Angew. Chem.* **2003**, *115*, 3407 – 3410; *Angew. Chem. Int. Ed.* **2003**, *42*, 3285 – 3288.
[15] R. Mathieu, R. Poilblanc, P. Lemoine, M. Gross, *J. Organomet. Chem.* **1979**, *165*, 243 – 252.
[16] H. Li, T. B. Rauchfuss, *J. Am. Chem. Soc.* **2002**, *124*, 726 – 727.
[17] J. D. Lawrence, H. Li, T. B. Rauchfuss, *Chem. Commun.* **2001**, 1482 – 1483.
[18] J. D. Lawrence, H. Li, T. B. Rauchfuss, M. Benard, M.-M. Rohmer, *Angew. Chem.* **2001**, *113*, 1818 – 1821; *Angew. Chem. Int. Ed.* **2001**, *40*, 1768 – 1771.
[19] CCDC-222734 (**1**) contains the supplementary crystallographic data for this paper. These data can be obtained free of charge via www.ccdc.cam.ac.uk/conts/retrieving.html (or from the Cambridge Crystallographic Data Centre, 12 Union Road, Cambridge CB2 1EZ, UK; fax: (+44) 1223-336-033; or deposit@ccdc.cam.ac.uk).
[20] Unexpectedly, addition of acid to solutions of the related phenyl-substituted comlex [(μ-ADT)$Fe_2(CO)_6$] (where R = phenyl) did not result in protonation of the bridge nitrogen atom, as evidenced by unchanged UV/Vis, IR, and NMR spectra.
[21] Acid titrations, monitored by electrochemical, UV/Vis, and IR techniques indicate that a slight excess of acid is required for exhaustive protonation of **1** (see the inset in Figure 2).
[22] All potentials are given versus Fc/Fc$^+$ and as differential pulse voltammetry peak potentials E_{pk}.
[23] A similar effect can be observed for the irreversible oxidation potential of **1**, which is shifted anodically by about 400 mV upon protonation and formation of **1H$^+$**.
[24] I. Bhugun, D. Lexa, J.-M. Savéant, *J. Am. Chem. Soc.* **1996**, *118*, 3982 – 3983.
[25] The different reference systems were compared by using [(μ-$S(CH_2)_3S)Fe_2(CO)_6$] as a calibrating agent, which is reduced at −1.16 V versus Ag/AgCl (F. Gloaguen, J. D. Lawrence, M. Schmidt, S. R. Wilson, T. B. Rauchfuss, *J. Am. Chem. Soc.* **2001**, *123*, 12518 – 12527). With our reference system and under otherwise identical conditions, this complex is reduced at −1.67 V, which gives rise to a ΔE value of 0.51 V.
[26] R. P. Bonar-Law, A. P. Davis, B. J. Dorgan, *Tetrahedron* **1993**, *49*, 9855 – 9866.
[27] P. F. Brandt, D. A. Lesch, P. R. Stafford, T. B. Rauchfuss, *Inorg. Synth.* **1997**, *31*, 112 – 116.

